scientific reports

Check for updates

OPEN

Molecular mechanisms at the basis of the protective effect exerted by EPPS on neurodegeneration induced by prefibrillar amyloid oligomers

Beatrice Zarrilli[1,2,12], Roberto Bonanni[3,12], Marcello Belfiore[4], Mariagrazia Severino[4], Ida Cariati[1], Raoul Fioravanti[5], Giacomo Cappella[4], Simona Sennato[6], Claudio Frank[7], Cristiano Giordani[8,9], Virginia Tancredi[1,10], Cecilia Bombelli[11], Marco Diociaiuti[11]✉ & Giovanna D'Arcangelo[1,10]

It has been shown recently, without an explanation of the possible molecular mechanisms involved, that 4-(2-hydroxyethyl)-1-piperazinepropanesulphonic (EPPS) acid effectively protects from the neurotoxicity induced by oligomers and plaques formed by the protein amyloid-β protein. Here we report the same protective effect, obtained in vitro (HT22-diff cell line) and ex vivo (hippocampal slices) models, against amyloid neurotoxicity induced by oligomers of salmon Calcitonin (sCT), which has been shown to be a good model for the study of neurodegenerative diseases. Based on biophysical studies focusing on the protein aggregation kinetic and the interaction of the aggregates with model membranes, we propose a possible molecular mechanism underlying the protective effects. Taken together, our results indicate that EPPS is able to counteract the direct association (primary aggregation) of harmless low-molecular weight aggregates (dimers and trimers) or their aggregation catalysed by surfaces present in the solution (secondary aggregation). Thus, EPPS stabilizes harmless aggregates and hinders the formation of toxic and metastable prefibrillar oligomers. Overall, our data demonstrate that EPPS is an excellent drug candidate for the treatment of neurodegeneration due to misfolded proteins, such as Alzheimer's or Parkinson's disease.

Keywords neurodegeneration, Alzheimer's disease (AD), salmon calcitonin (sCT), 4-(2-hydroxyethyl)-1-piperazinepropanesulphonic acid (EPPS), Prefibrillar Oligomers (PFOs)

Neurodegenerative diseases, such as Alzheimer's disease (AD), Parkinson's disease (PD) and other less frequent such Huntington's (HD), Prion (Pr) and dementia with Lewy bodies diseases[1,2], are a heterogeneous class of severe and incurable disorders[3] characterized by the progressive loss of structure and function of neurons[4]. Among these, some are particularly frequent and include AD and PD (AD today affects approximately 5% of people over 60 years old and in Italy there are an estimated 500 thousand sufferers), other are rare diseases such

[1]Department of Systems Medicine, "Tor vergata" University of Rome, Via Montpellier 1, 00133 Rome, Italy. [2]Laboratory of Experimental Neurology, IRCCS Fondazione Santa Lucia, Rome, Italy. [3]Department of Biomedicine and Prevention, "Tor vergata" University of Rome, Via Montpellier 1, 00133 Rome, Italy. [4]National Centre for Drug Research and Evaluation, Istituto Superiore di Sanità, Rome, Italy. [5]Department of Infectious Diseases, Istituto Superiore di Sanità, Rome, Italy. [6]CNR - Institute of Complex Systems (ISC) - Sede "Sapienza", c/o Physics Department, "Sapienza" University of Rome, 00185 Rome, Italy. [7]UniCamillus - Saint Camillus International University of Health Sciences, Via di Sant'Alessandro 8, Rome 00131, Italy. [8]Instituto de Física, Universidad de Antioquia, Calle 70 No. 52-21, 050010 Medellín, Colombia. [9]Grupo Productos Naturales Marinos, Facultad de Ciencias Farmacéuticas y Alimentarias, Universidad de Antioquia, Calle 70 No. 52-21, 050010 Medellín, Colombia. [10]Centre of Space Bio-Medicine, "Tor vergata" University of Rome, Via Montpellier 1, 00133 Rome, Italy. [11]CNR - Institute for Biological Systems, Secondary Office of Rome - Reaction Mechanisms c/o Chemistry Department, "Sapienza" University of Rome, Rome, Italy. [12]Beatrice Zarrilli and Roberto Bonanni, Marco Diociaiuti and Giovanna D'Arcangelo contributed equally to this work. ✉email: marco.diociaiuti@iss.it

as Prion's Protein disease and the large family of polyglutamine diseases (United Europe defines "rare disease" when its prevalence is below 0.05% ofthe population).

Despite the great and many differences in clinical manifestation and incidence, neurodegenerative diseases share several characteristics such as increasing occurence with age and chronic and progressive nature[2,5–7].

It's now generally accepted that many disorders are related to the misfolding and the following aggregation of the specific proteins involved, called amyloid proteins. Seven of the 37 proteins associated with amyloid disease form deposits in the CNS, giving rise to severe neurodegenerative conditions such as AD and PD[6]. The Central Nervous System (CNS) seems a suitable environment and this could be due to neurons that, compared to other cell types, are especially susceptible. Infact, due to their long lifetime, when damaged they are not readily replenished through cell division.

Normally, misfolded proteins are degraded inside the cell in proteasomes or outside the cell by macrophages[8]. In amyloidosis, a condition associated with various hereditary and inflammatory diseases[9], these control mechanisms are less efficient and, therefore, cause misfolded proteins to accumulate outside the cells[10], where are deposited as fibrils in extracellular spaces[11].

Amyloid proteins do not have any evident similarity in their primary structures; however, they share a typical aggregation behaviour, proceeding through several steps, which include the formation of Prefibrillar Oligomers (PFOs), Annular or Linear Protofibrils (APFs or LPFs) and Proto/Mature Fibres (MFs)[12,13].

The fibrillar deposits might not be responsible for the neurotoxic effects and memory loss of these disorders[5]. In fact, it is now generally accepted that small soluble oligomers are more toxic than MFs, which are considered almost inactive or even protective, due to their ability to subtract soluble toxic species[14,15]. Metastable and soluble PFOs show surprising commonalities in their structure and biological activity[7,16].

In general, neuronal damage caused by PFOs starts with the alteration of Ca^{2+} homeostasis due to the permeabilization of membranes and a consequent common chain of events leading to the neuron dead[17,18]. Several mechanisms of membrane permeabilization have been proposed such as the formation of "amyloid pores" by protein aggregates mimicking the action of bacterial toxins or the direct rupture due to mechanical action[16].

It follows that the strategy most commonly used in the design of drugs against neurotoxicity is to reduce the abundance of the toxic species, which are the soluble metastable PFOs. Several approaches have been proposed to interfere with one of the two main pathways of PFOs formation: direct aggregation of monomers (primary nucleation) and indirect aggregation catalyzed by the surface of existing MFs (secondary nucleation)[19] and/or the neuron surfaces[20].

A first way to obtain the reduction of the metastable and toxic PFOs number, could be to inhibit their formation from monomers (primary nucleation) and/or to disassemble the pre-formed ones.

Above a critical fibril concentration, the "secondary nucleation" seems to be the most effective PFOs source and to this aim, several monoclonal antibodies have been developed[21]. Aducanumab was able to inhibits the "secondary nucleation" by coating the MFs surface[22] and seemed to be successful. Unfortunately, there is a lot of concern and prudence about the real clinical efficacy of this drug and on secondary effects[23] and it has been withdran from the market in 2024.

Recently, Lecanemab, which is a monoclonal antibody specifically designed to bind protofibrils[24], showed encouraging effects when used since the early onset of the disease. However, although characterized by less severe side effects, on 26 July 2024 the European Medicine Agency (EMA) has recommended the refusal of the marketing authorisation for this antibody (Lecanemab). The most important safety concern the occurrence in some patients of serious events, including large bleeds in the brain which required hospitalisation[25]. Other investigations are in progress[26].

Thus, the use of monoclonal antibodies is not free of dangerous side effects. Moreover, the use of monoclonal antibodies is very expensive. In fact, a cycle of treatment with Aducanumab can cost up to 56,000 USD, and this strongly reduces the possibility of cure in many countries and in some parts of the population.

All these considerations justify the interest in the identification of new molecules able to reach the same targets. Interestingly, on 2015 Kim et al., in a significant paper published in Nature Communications[27], showed that 4-(2-hydroxyethyl)-1-piperazinepropanesulfonic acid (EPPS), a small (MW of 252.33 Da) and cheap molecule (few €/gr) commonly used for the preparation of buffers in biological applications[28], was able to rescue hippocampus-dependent cognitive deficits in APP/PS1 mice. Notably Kim et al.[27] showed that this important goal was achieved by the effective disaggregation of Aβ-oligomers and plaques and that EPPS was harmless in its biological models.

Unfortunately, Kim et al. didn't investigate the molecular mechanisms at the basis of this protective effect, mechanisms that, in our opinion, would be important to know both to understand the basis of neurodegeneration even more thoroughly and to design effective drugs.

Therefore, the aim of our study was to evaluate the protective effects exerted by EPPS against the amyloid neurotoxicity induced by PFOs and to investigate on the nature of the molecular mechanisms at the basis of the process. To reach this aim we used several consolidated models: salmon Calcitonin (sCT) as an amyloid protein, differentiated HT-22 cell line as neuron model, murine hippocampal slices as learning and memory model and liposomes as neuronal membrane model.

sCT is a polypeptidic hormone secreted by the parafollicular C cells of the thyroid gland, belongs to the amyloid family and, unlike other members of the family, is characterized by the longest aggregation lag-phase among CT variants[28]. For this reason, in the past we were able to prepare native and stable sample rich in sCT-PFOs of low molecular weight to be tested onto cells. We successfully used sCT as a tool to investigate the amyloid neurotoxicity since the very early stages[29,30]. We have shown that, among various sCT aggregates, only sCT-PFOs and not proto- and mature-fibres, were neurotoxic[15,31]. In a biophysical study we demonstrated that the membrane damage and the consequent Ca^{2+}-influx was the molecular mechanisms leading to neurotoxicity[13].

Eventually, we proposed an innovative amyloid neurotoxicity mechanism where the two pre-existing and alternative paradigms, the "membrane permeabilization" and the "receptor-mediated", must coexist: sCT-PFOs only weakly damaged the neurons membranes enough to trigger strong NMDA-mediated Ca^{2+}-influx leading to Long-Term-Potentiation (LTP) impairment and neurotoxicity[32].

We successfully used differentiated HT22 (HT22-diff) as neuronal model[32]. HT22 cells were used because they acquire properties similar to those of mature hippocampal neurons in vivo when they differentiate[33].

We also performed electrophysiology experiments in murine hippocampal slices, which are a widely used model of learning and memory. In particular, experiments were performed recording, in the CA1 region, the Basal Synaptic transmission (BST) and the LTP, which are known to be an index for assessing synaptic plasticity[32].

In this paper, we report on experiments performed on the biological models used before, but in the presence of EPPS. Moreover, to focus on the molecular mechanisms at the basis of the effects of EPPS, we used membrane models studied by biophysical techniques.

The use of membrane models has remarkably improved the knowledge on the biochemistry of amyloid proteins interacting with lipids. Although very simplified compared to the actual neuronal membrane, lipid bilayers can be prepared and liposomes are the most used model[34]. Recently, the attention has been focused on the so-called "lipid-rafts", which are nano-domains featuring peculiar composition and functions: they are rich in cholesterol (Chol), sphingolipids and membrane proteins, and are responsible for signal transduction, neuronal differentiation and the entrance of pathogens and toxins into the cell[35]. Moreover, lipid rafts are involved in neurodegeneration because they have been shown to promote on one side the aggregation of amyloid proteins into oligomers and fibers and, on the other, the formation of membrane pores. Simplified models for lipid-rafts were proposed, based on the observation that detergent-resistant membranes obtained from actual cellular membranes were rich in sphingolipids and Chol and depleted in unsaturated phosphatidylcholines. Moreover, biophysical studies indicated that liposomes formulated with sphingolipids and Chol in ordered phases, such as liquid- or solid-ordered, were found to be resistant to solubilisation with Triton X-100, while soluble if in liquid-expanded. GM1/Chol/POPC mixtures mimicking the local composition of lipid-rafts in the cellular membrane are presently used as raft models[36,37]. On 2019 we demonstrated that an anionic ganglioside, called GM1, played a crucial role in the interaction of sCT-PFOs aggregates with the membrane and triggers the formation of amyloid pores[13].

Based on the previous consideration, to study the interaction between the sCT species and the neuronal membrane, we decided to use liposomes mimicking both the whole neuronal membrane (with a low content of GM1) and/or the lipid-rafts present on the surface of the plasma membrane (with a high content of GM1).

To investigate the interaction occurring between sCT-PFOs and model membranes, we applied the Laser Doppler Electrophoresis technique to determine the Z-potential. It was possible to measure the electrophoretic mobility of the charged species present in the suspension (sCT aggregates and liposomes) and get information on the state of charge at the surface, in the absence or presence of EPPS[38].

Finally, to study the effect induced by EPPS on the aggregation kinetics of sCT and its capability to disaggregate amyloid mature fibres, we performed ThT experiments.

Results

Preparation and characterization of non-aggregated (sCT-NA), PFOs (sCT-PFOs) and protofibers (sCT-Fs) samples. Evaluation of the effects induced by EPPS

To prepare oligomeric species enriched samples, an aggregated 1 mM sCT solution (obtained as described in detail in Sect. 4.3) was loaded in the SEC column. The obtained MW profile, obtained by the calibration standards elution profile (Fig.S1 of SI), is shown in Fig. 1A (black) and was characterized by: (i) a main peak that included monomers, dimers, trimers and tetramers, even though dimers and trimers were the most abundant; (ii) a secondary peak, at a MW of about 100 kDa, corresponding to proto-fibers (made of more than 30 monomers). We used the central fractions of the main peak as a representative sample of PFOs and the secondary one of proto-fibers (Fs).

The column didn't give a useful peak relative to monomers but only a shoulder, likely due to their metastable nature. For this reason, we decided to prepare native non-aggregated (NA) sCT solutions, representative of samples rich in very low molecular weight aggregates, by dissolving, just before use, the freezed solutions (prepared in desalinated water as described in Sect. 4.3) in PB (5mM) at a final concentration of 80 μM, which was the typical concentration of the samples eluted from the column.

In order to investigate by SEC the effect exerted by EPPS, we incubated sCT as described in Sect. 4.3 but in the presence of EPPS, at a relative molar concentration of 1 sCT per 375 EPPS (used in the following biological tests). The obtained MW profile, obtained by the calibration standards elution profile (Fig. S2 of SI), is shown in Fig. 1A (red) and was characterized by a single and sharp peak, clearly shifted towards low MWs close to monomers. The peak is asymmetric, with shoulders at high MWs including dimers and trimers. The peak relative to Fs completely disappeared. Notably, EPPS strongly modified the aggregation process of sCT, avoiding the formation of the metastable and toxic PFOs (tetramers and higher) and inhibiting the formation of proto-fibres (Fs).

The characterization of the samples used in the following experiments, representative of the various aggregates (NA, PFOs and Fs), has been also obtained by the PICUP procedure followed by tricine SDS-PAGE (Fig. 1B and Fig.S3). The PICUP procedure, developed by Fancy and Kodadek[39] and applied by Bitan to the study of metastable protein[40], was applied before the gel analysis to fix metastable aggregates in their original configurations, which could be lost in the reducing SDS-PAGE buffer.

Concerning the PFOs solution, the gel analysis showed the presence of bands relative to dimers, trimers, tetramers, pentamers, hexamers, heptamers and octamers (lane 3). Monomers were practically absent.

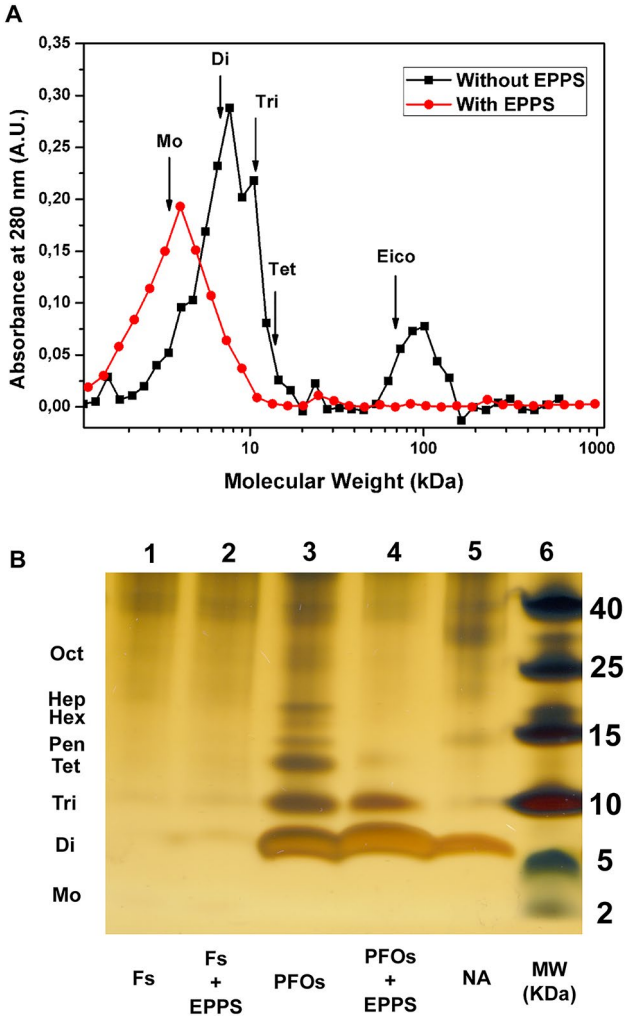

Fig. 1. (**A**) Size Exclusion Chromatography (SEC) Molecular Weight (MW) profiles of the sCT native sample 1 mM incubated for 24 h at room temperature whitout (black) and with (red) EPPS at 375 mM. The calibrations of the two G50 columns are reported in the SI. The theoretical MWs relative to the different sCT species (Monomer – Mo; MW 3.432 kDa and their multiples) are also indicated. (**B**). Electrophoresis GEL relative to sCT samples (SDS-PAGE after the PICUP procedure) rich in proto-Fibres (Fs - lane 1), Pre-Fibrillar-Oligomers (PFOs - lane 3) and Non-Aggregated (NA - lane 5), with and without EPPS (3 mM).

Concerning the sample rich in Fs, the gel analysis didn't give well-defined bands (lane 1), likely due to the high MW of the protofibres (100 kDa), which didn't enter the gel.

In the case of NA sample, we can see that dimer was the most abundant species (lane 5). Trimers, pentamers and octamers were also present, but with abundances non comparable to those observed in the PFOs solution (pentamers, hexamers, heptamers and octamers) (lane 3). Even in this case, monomers were not detected. This is in agreement with the NMR results published for non-aggregated sCT by Andreotti and Motta[41] indicating that, at pH 7.3, dimer is the stable form.

We decided to use the three sCT samples as representative of the different species: proto-fibers (sCT-Fs), PFOs (sCT-PFOs) and non-aggregated (sCT-NA).

Finally, we investigated by the PICUP procedure followed by tricine SDS-PAGE, the effect induced by the EPPS treatment, for 24 h at the concentration used in our biological experiments (3 mM), on the sCT-PFOs and sCT-Fs samples.

Concerning sCT-PFOs, only two well-defined bands relative to dimers and trimers were obtained even if a faint one relative to tetramers, can be observed (lane 4). This result indicated that, after 24 h, EPPS was able to disaggregate the metastable and toxic PFOs formed during the aggregation process performed during the sample preparation, well visible in lane 3.

Concerning sCT-Fs, we didn't note any significant change induced by EPPS (lane 1 and 2). This indicated that the pre-formed mature protofibres of MW of about 100 kDa, didn't enter the gel due to their big MW, in both cases.

Protective effects of treatment with EPPS against the damage induced by sCT-PFOs on HT22 differentiated cells

To identify a non-toxic EPPS concentration, we constructed a Dose-Response curve by treating differentiated HT22 cells with increasing concentrations of the test substance for 1 h and then we assessed cell viability by means of 3-(4,5-dimethylthiazol-2-yl)-5-(3-carboxymethoxyphenyl)-2-(4-sulfophenyl)-2 H-tetrazolium (MTS) assay. We decided to perform the treatment for 1 h because in the following hippocampal slice experiments, the treatments can be done at maximum for 1 h.

Results are reported in Fig. 2A and, as it can be observed, EPPS didn't lead to a reduction in cell survival at concentrations between 0.5mM and 5mM, whereas at a concentration of 241 ± 34 mM, EPPS leads to a reduction in survival of 50%. This value is considered the half maximal Inhibitory Concentration (IC50). Finally, EPPS

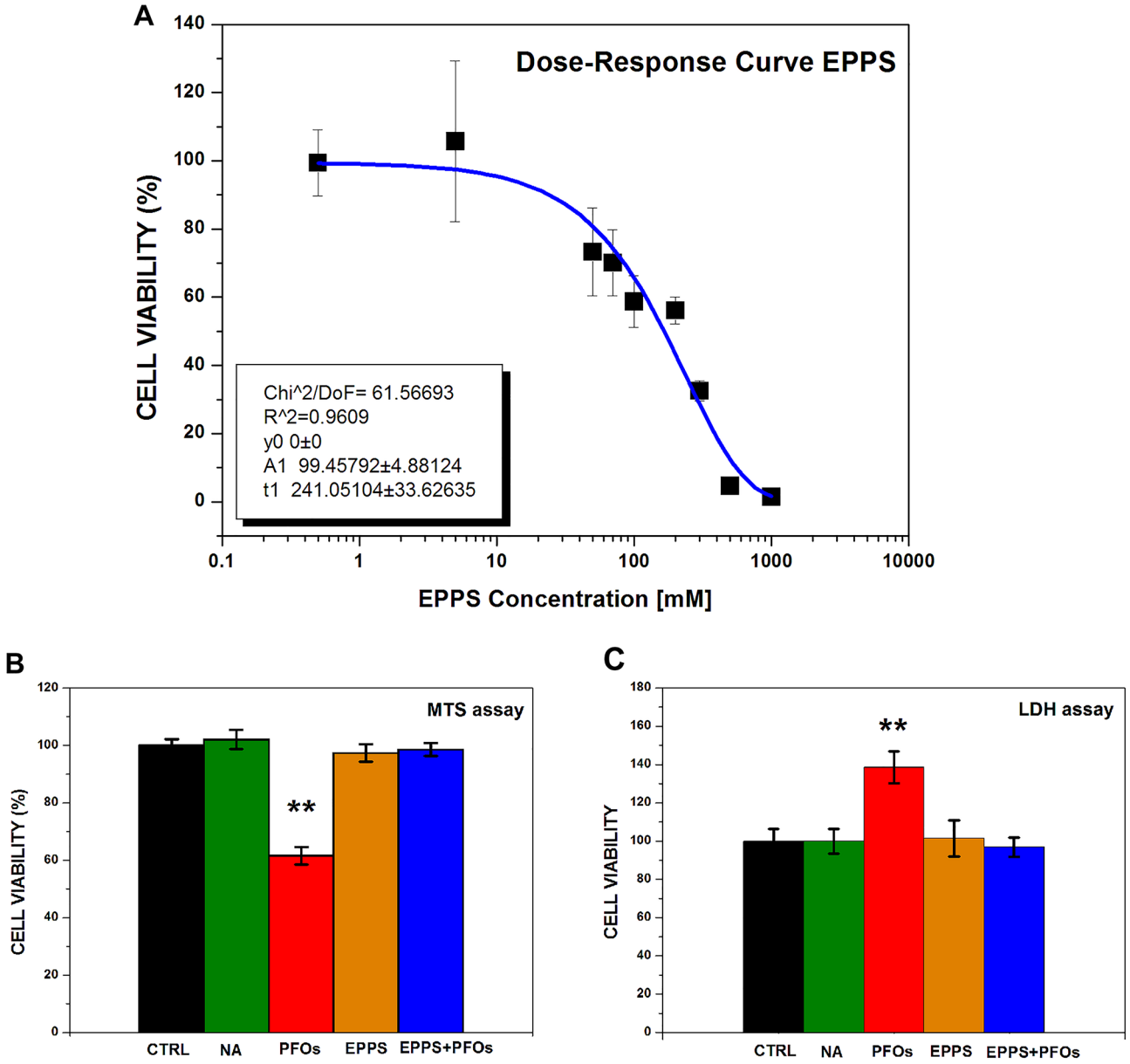

Fig. 2. (**A**) Dose-Response curve (MTS assessment) obtained after 1 h of EPPS treatment, in differentiated HT22 cells. In the concentration range between 0.5mM and 5mM, cell viability is not affected and it reachs the half-maximal Inhibitory Concentration (IC50) at 241 ± 34 mM. (**B**) Biological effects induced on differentiated HT22 cells by 24 h of EPPS different treatments evaluated by the MTS assessment: in green, with sCT-NA (8μM) solution ($n = 15$ wells from $N = 4$ experiments); in red to test the PFOs toxicity, with sCT-PFOs (8μM) ($n = 22$ wells from $N = 6$ experiments) (**$p < 0.01$ with respect to CTRL in black,); in brown to validate the Dose-Response curve obtained after only 1 h of EPPS treatment, with EPPS (3mM)($n = 3$ wells from $N = 2$ experiments); in blue to test the EPPS protection effect, with EPPS (3mM) + PFOs (8μM) ($n = 17$ wells from $N = 5$ experiments). (**C**) The same biological effects, evaluated by LDH assessment (in the ordinate axis the Relative Luminiscence Unit % is indicated).

concentrations above 500mM were associated with a complete loss of cell survival. Thus, we consider that, below 5mM, EPPS has non-toxic effect after 1 h of treatment. To verify the non-toxic effect of EPPS at concentration below 5mM, even after 24 h of treatment, we performed a specific cytotoxicity experiment treating HT22 differentiated cells with 3mM EPPS for 24 h. We evaluated EPPS toxicity by two different tests: MTS, which is a metabolic test based on the mitochondrial activity and lactate dehydrogenase (LDH), which is a non-metabolic test whose positivity indicates cell damage. The results (brown columns in Fig. 2B,C) clearly demonstrated that EPPS was non-toxic after 1 h and 24 h of treatment, in both tests.

Based on the results of our EPPS Dose-Response curve and toxicity tests, and the experiments conducted by Kim et al.[27], we decided to investigate the effects of 24 h of treatment with EPPS (3mM) on the cytotoxicity exerted by sCT-PFOs on HT22 differentiated cells.

Results relative to the biological effects, evaluated by the MTS assay, exerted by EPPS (3mM) are reported in Fig. 2B. As it can be seen, the treatment with 8μM sCT-PFOs (in red) resulted in a significant reduction (approximately 40%) of cell survival ($^{**}p < 0.01$), when compared to the control condition (CTRL, in black) while treatment with sCT-NA, at the same concentration, did not lead to a reduction in cell viability, in good agreement with results reported by Cariati et al.[42]. It is relevant to observe that the combined treatment with EPPS (3mM) + sCT-PFOs (8μM) (in blue) didn't reduce cell survival compared to the control condition and caused a complete recovery of cell viability, compared to treatment with PFOs. Thus, EPPS had a protective effect against the damage induced by sCT-PFOs.

The LDH results confirmed the MTS assay (Fig. 2C). In fact, a significant increase of LDH enzyme in cells treated with sCT-PFOs (8μM) is observed, demonstrating the high PFOs cytotoxicity. Otherwise, cells treated with EPPS (3mM) + sCT-PFOs showed values similar to the control.

All our cytotoxcitity results demonstrated the strong protective effects of the EPPS treatment against the amyloid toxicity induced in vitro by sCT-PFOs.

Protective effects of treatment with EPPS against the damage induced by sCT-PFOs on murine hippocampal slices

To physiologically assess the protective effects of EPPS, in terms of baseline transmission (BST) and on Long-Term-Potentiation (LTP), we carried out electrophysiology experiments and measured population spike (% PS) in murine acute hippocampal slices. Based on the results of the cell viability experiments reported below, we decided to administer EPPS at a concentration of 3mM. Figure 3 shows the electrophysiological spectra of the different treatments we performed.

We initially verified the control condition (CTRL), working with slices in artificial cerebral spinal fluid (aCSF) solution where we didn't administer any substance (black trace). A stable BST, a proper enhancement after tetanic stimulation and a LTP establishment, can be observed.

At minute 17 (first arrow), slices were treated with:

(i) EPPS, maintained for 60 min up to the induction of the tetanic stimulus (minute 77, third arrow) (orange trace);
(ii) EPPS, maintained for 40 min up to the administration of the mixture EPPS + PFOs (minute 57, second arrow), which was maintained up to the induction of the tetanic stimulus (minute 77, third arrow) (blue trace);
(iii) plain aCSF solution, maintained for 40 min up to the administration of the sCT-NA solution (minute 57, second arrow), which was maintained for 20 min up to the induction of the tetanic stimulus (minute 77, third arrow) (green trace);
(iv) plain aCSF solution, maintained for 40 min up to the administration of the PFOs solution (minute 57, second arrow), which was maintained for 20 min up to the induction of the tetanic stimulus (minute 77, third arrow) (red trace).

PS amplitude values, for each group of hippocampal slices, were recorded from the beginning up to 170 min and are reported in Table 1.

As previously reported by our group, sCT-PFOs resulted to be toxic[32]. In fact, the treatment with plain sCT-PFOs (red) induced a strong reduction in LTP with PS values that reached values similar to those of BST 170 min after the high-frequency stimulation (HFS) (Fig. 3; Table 1: row 6). However, in this case we didn't observe any significant alteration in the BST with respect to the CTRL (inset of Fig. 3; Table 1: row 3).

The treatment with sCT-NA solutions (green) didn't alter either BST or LTP (Fig. 3; Table 1: row 3 and 6). This confirmed that the toxic aggregates (pentamers, hexamers and heptamers) were not abundant in this solution.

Concerning the effects of EPPS, we can say that its presence induced an increase in the BST, without alterations of LTP. In particular, we observed (inset of Fig. 3) a significant increase of the PS amplitude values when EPPS was present, alone or together with PFOs (Fig. 3: Table 1: row 3). This didn't generate an epileptic tendency, which is known to induce an increase in BST[42]. Notably, the presence of EPPS not altered the LTP, immediately before the tetanic stimulus or at long term (Fig. 3; Table 1: row 4 and 6).

Finally, the treatment with EPPS + sCT-PFOs induced a significant recovery of the LTP response that was strongly inhibited by the administration of the toxic sCT-PFOs.

The results of electrophysiology demonstrated, in agreement with the previously reported findings of cytotoxicity experiments, the strong protective effects of the EPPS treatment against the amyloid toxicity induced by sCT-PFOs.

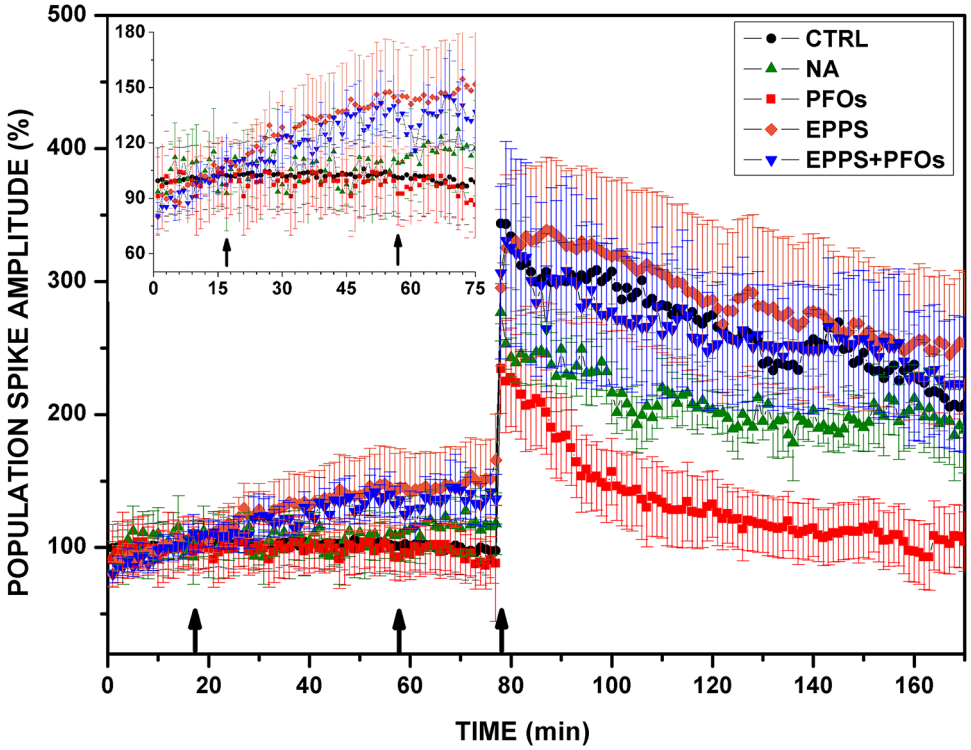

Fig. 3. Synaptic plasticity in CA1 subfield of mouse hippocampal slices. Spectra relative to LTP induced in hippocampal brain slices by PFOs (red) ($n=6$) and NA solutions (green) ($n=6$), EPPS solution (orange) ($n=10$) and EPPS + PFOs solution (blue) ($n=6$), compared to untreated samples (CTRL in black) ($n=6$). The first arrow from the left represents the starting point of the EPPS treatments, when performed (EPPS and EPPS + PFOs). The second arrow represents the administration of NA, PFOs and PFOs + EPPS solutions, which were maintained (20 min.) up to the tetanic stimulations (third arrow). The insert (top, left) shows in detail the BST.

Time (min)	CTRL (PS% Amplitude)	sCT-NA (PS% Amplitude)	sCT-PFOs (PS% Amplitude)	EPPS (PS%Amplitude)	EPPS + sCT-PFOs (PS% Amplitude)	Significance between groups at different times
12–16	101.1 ± 5.8	102.8 ± 8.4	99 ± 8.2	103.8 ± 6.7	100.3 ± 3.7	no significance
52–56	102.9 ± 7.7	101.6 ± 7.7	99.7 ± 7.9	144.8 ± 11.7	137.4 ± 6.3	CTRL vs. EPPS, $*p<0.05$; NA vs. EPPS, $*p<0.05$; PFOs vs. EPPS, $**p<0.01$
73–77 Before HFS	98.3 ± 7.5	116.4 ± 9.9	88.3 ± 7.5	182.6 ± 16.9	170.7 ± 18.6	CTRL vs. EPPS, $***p<0.001$; CTRL vs. EPPS + PFOs, $*p<0.05$; NA vs. EPPS, $*p<0.05$; PFOs vs. EPPS, $***p<0.001$; PFOs vs. EPPS + PFOs $**p<0.01$
80–84 After HFS	318.6 ± 14.2	242.0 ± 7.5	216.2 ± 15.8	330.9 ± 24.7	308.7 ± 27.8	CTRL vs. PFOs, $*p<0.05$; NA vs. EPPS $*p<0.05$; PFOs vs. EPPS $***p<0.001$; PFOs vs. EPPS + PFOs $*p<0.05$
140–144	261.3 ± 10.3	188.9 ± 6.1	109.3 ± 8.9	267.2 ± 19.7	255.9 ± 20.3	CTRL vs. PFOs, $**p<0.001$; NA vs. PFOs, $*p<0.05$; NA vs. EPPS, $*p<0.05$; PFOs vs. EPPS, $**p<0.001$; PFOs vs. EPPS + PFOs, $**p<0.001$
166–170	221.6 ± 10.0	192.1 ± 12.8	106.6 ± 10.1	250.9 ± 18.9	222.8 ± 20.6	CTRL vs. PFOs, $**p<0.001$; NA vs. PFOs, $*p<0.05$; PFOs vs. EPPS, $**p<0.001$; PFOs vs. EPPS + PFOs, $**p<0.001$

Table 1. Percentage of PS amplitude values of BST and LTP recorded in the CA1 region of hippocampal slices from the control group and groups treated with different substances at different times. *PS* population spikes, *BST* basal synaptic transmission, *LTP* long-term potentiation, *CTRL* control group, *EPPS* 4-(2-hydroxyethyl)-1-piperazinepropanesulfonic acid, *PFOs* prefibrillar oligomers. $*p<0.05$; $**p<0.01$; $***p<0.001$.

Electrostatic properties of sCT species, and effects of EPPS in the sCT-liposome interaction

Z-potential experiments were performed on the three representative samples: sCT-NA, sCT-PFOs and sCT-Fs. The effect induced by the presence of 3mM EPPS (the same concentration used in the biological experiments) on the Z-potential of the sCT species, was also investigated.

Moreover, to study the interaction of the sCT species with membrane models, measurements were performed on samples containing a mixture of sCT and liposomes mimicking (i) the whole neuronal membrane, made of GM1, Chol and DPPC, with low content of the charged molecule GM1 (4, 48, 48 mol %); (ii) "lipid-rafts", with high content of GM1, made of GM1, Chol and POPC (50, 25, 25 mol%).

Finally, to investigate the mechanisms underlying the capability of EPPS to inhibit the toxic effects of PFOs, experiments were performed also in the presence of this substance (3mM). The Z-potential values, measured in at least three independent experiments, are reported in Table 2; Fig. 4.

The Z-potential of the sCT species

We observed that all Z-potential values were negative and, interestingly, that the aggregation state of the protein strongly affected the measured values. In particular, sCT-NA was weakly negative (-6 mV), sCT-PFOs was the less negative (− 1.6 mV) and sCT-Fs was the most negative (-30 mV) (Table 2, line 1–3).

Notably, the presence of EPPS in the solution strongly affected the Z-potential value of the sCT-NA (-10 mV) while did not affect the values relative to sCT-PFOs and sCT-Fs (Table 2, line 1–3 column 4). These effects were maintained over time.

The Z-potential of the liposomes

We observed that the composition of liposomes dramatically influenced the Z-potential values. As expected, a small number of GM1 exposing their negative group to the solvent, gave rise to weakly negative Z-potential values, difficult to measure and insensitive to the presence of any sCT species (Table 2, line 4). Conversely, the higher amount of GM1 gave rise to strongly negative values (around − 17 mV), in good agreement with results previously published by our group[43] (Table 2, line 5). The last condition, far from the electroneutrality conditions seen for low concentrations of GM1, is the more favorable to investigate variations induced by the interaction with the sCT molecules.

The Z-potential of the mixtures sCT-liposome with high content of GM1

In the absence of EPPS, each sCT species affects to a different extent the Z-potential of the plain liposomes (Table 2, line 6–8 column 2): the strongly negative value of plain liposomes (-17 mV) was considerably made less negative by the presence of sCT-NA (-7 mV) and sCT-PFOs (-10 mV) while was totally unchanged by sCT-Fs (-17 mV) (column 2). This observation suggests that species occurring in the sCT-NA and sCT-PFOs solutions bind to the membrane reducing its negative net charge, while the strongly negative sCT-Fs don't bind.

Notably, the presence of EPPS totally inhibited the effect induced by the sCT-NA solutions. In fact, the Z-potential of the mixtures in the presence of EPPS (-18 mV) (Table 2, line 6 column 3) is the same as plain liposomes without sCT-NA (-17 mV). This observation suggests that EPPS counteracted the binding to membranes of dimers and monomers occurring in the sCT-NA solutions. Conversely, EPPS didn't affect the Z-potentials induced on liposomes by the presence sCT-PFOs and sCT-Fs (Table 2, line 7–8 column 3).

Sample	Without EPPS Z-potential (mV)	With EPPS Z-potential (mV)	Variation induced by EPPS (mV)
sCT-NA	-5.9 ± 0.6	-14.1 ± 3.7	-8.2 **Maximun Effect**
sCT-PFOs	-1.6 ± 0.4	-0.4 ± 0.9	+ 1.2 **No Effect**
sCT-Fs	-28.6 ± 1.9	-31.4 +/-1.8	-2.8 **No Effect**
Lipo low GM1	-6.2 ± 0.6	-7.6 ± 0.8	-1.4 **No Effect**
Lipo high GM1	-16.3 ± 1.9	-17.7 ± 1.2	-1.4 **No Effect**
Lipo high GM1 + sCT-NA	-9.2 ± 1.3	-16.8 ± 1.7	**-7.6** **Maximum Effect**
Lipo high GM1 + sCT-PFOs	-9.8 ± 1.1	-7.4 ± 0.7	+ 2.4 **No Effect**
Lipo high GM1 + sCT-Fs	-17.7 ± 2.5	-18.7 ± 1.7	-1 **No Effect**

Table 2. Z-potential values of sCT species, plain liposomes, and the mixture of liposomes with high GM1 content and sCT species in the absence (column 2) and in the presence (column 3) of EPPS. Each value is the mean of at least 3 independent experiments and a difference of about ± 3.5 in column 4, was not considered meaningful (within the experimental errors). Column 4 highlights the effects induced by EPPS. The sCT concentration of all samples was normalized at about 30mM.

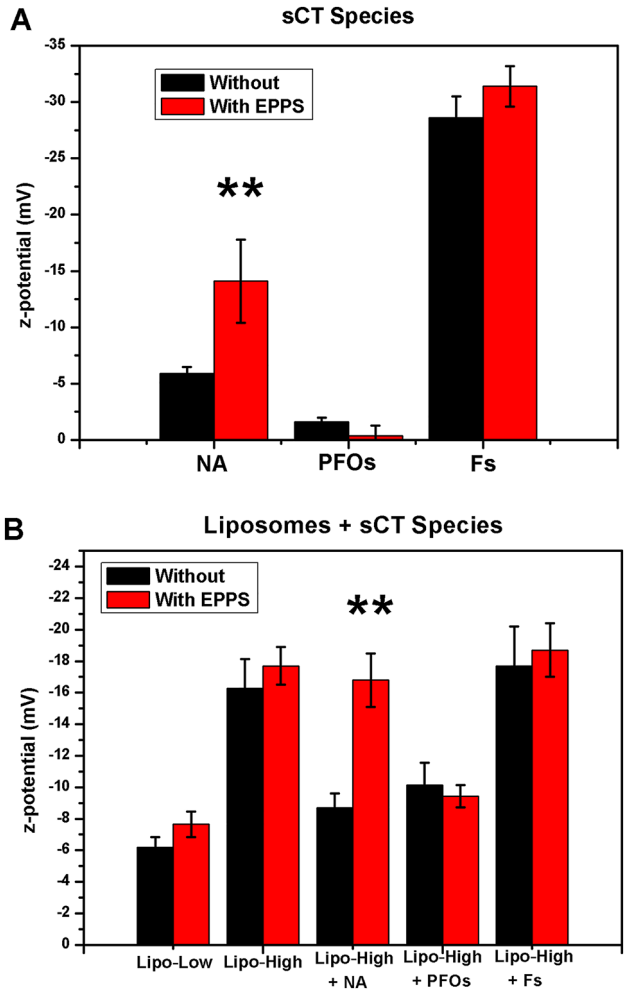

Fig. 4. Results of Z-potential experiments on (**A**) sCT species, and (**B**) plain liposomes (high and low GM1 content) and mixture of liposomes with high GM1 content with sCT species in the absence (black) and in the presence (red) of EPPS (3mM). Each value is the mean of at least 3 independent experiments. **Indicates statistical significance.

To summarize, the results of the Z-potential experiments highlighted that EPPS had a strong interaction only with sCT-NA solutions and was able to inhibit the interaction of the sCT aggregates present in these samples (dimers and trimers) with the neuronal membrane model.

Effects of the EPPS on the sCT aggregation and disaggregation tests

To investigate the capability of EPPS to inhibit the aggregation kinetics of the amyloid proteins and/or disaggregate pre-formed mature fibres, we performed ThT experiments.

As it can be observed in Fig. 5A, the aggregation kinetics of 1 mM sCT was not affected by 3mM EPPS; otherwise at 20mM EPPS the aggregation kinetics resulted strongly modified but not inhibited. Notably, higher EPPS concentrations totally abolished the protein aggregation. We underline that the previously reported biological experiments were performed at 375 EPPS per 1 sCT molecules (8μM of sCT with 3mM of EPPS), which is under conditions where protein aggregation is completely inhibited.

Concerning the disaggregating effect of EPPS on pre-formed sCT-Fs, in Fig. 5B it's evident that, after more than 1 month, the EPPS was not able to effectively disaggregate the well-formed fibres obtained at the end of the aggregation experiment (that is after about 8 days of incubation); only a small (about 20%) but statistically significant (t-test value of 1.42×10^{-6}) reduction of the β-structures can be observed after 720 h. Conversely, after 24 h of incubation, which is the treatment in the biological experimets, significant reduction cannot be detected (t-test value of 0.75209).

Discussion and conclusions

To evaluate the protective effects exerted by EPPS against PFO-induced amyloid neurotoxicity and try to clarify the molecular mechanisms underlying these protective effects, we exploited in vitro (HT22-diff cell line), ex vivo (hippocampal slices) and liposomal membrane models, performing cytotoxicity, electrophysiology and

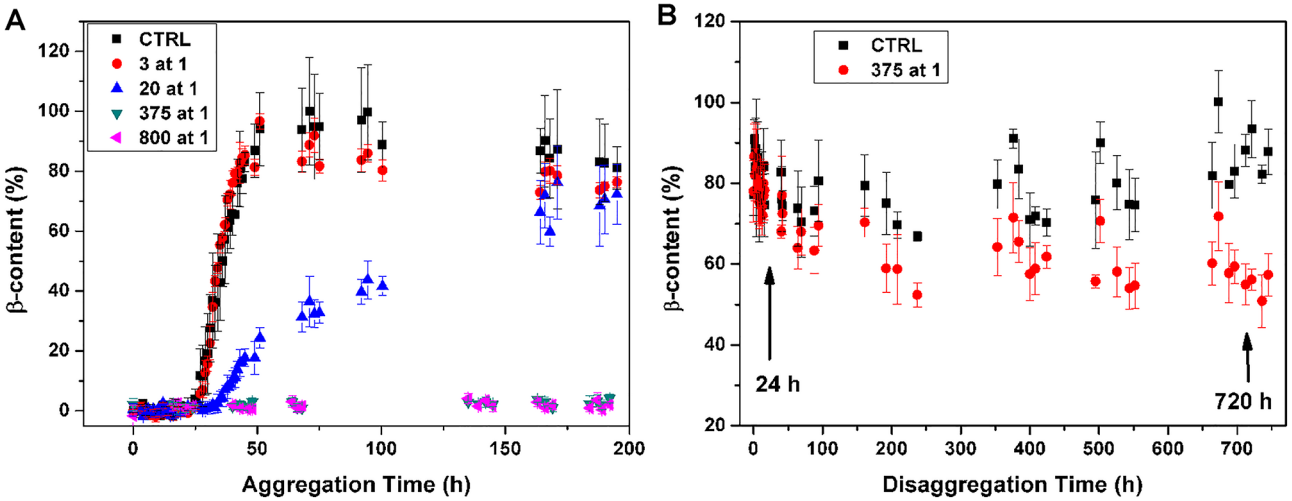

Fig. 5. (**A**) the typical aggregation curve of sCT at room temperature at 1mM concentration in PB (5mM) in the presence of EPPS at increasing molar concentrations. (**B**) the effects of 375mM EPPS on the fully fibrillated sCT samples obtained after more than 8 days of incubation (CTRL of A). All values are normalized at the maximum florescence value, obtained in the aggregation experiment after 71 h. T-test indicates no-difference after 24 h ($t = 0.75209$) and significant difference after 720 h of incubation ($t = 1.42 \times 10^{-6}$).

electrostatic interaction experiments. We also correlated the results of the biological experiments with the characterization of the amyloid sCT samples performed by SDS-PAGE and SEC analysis.

The results of the cytotoxicity tests on HT22-diff cells showed that an EPPS concentration below 10mM didn't cause any toxic effect (Fig. 2A). Thus, we considered that, at a concentration of 3mM, EPPS can be used as a protective substance without side effects; therefore we tested the efficacy of EPPS at this non-toxic concentration against the neurotoxicity induced by the amyloid sCT-PFOs.

The toxicity induced by the sCT-PFOs and sCT-NA samples in differentiated HT-22 cell line, is reported in Fig. 2B and C. As expected, sCT-PFOs induced a 40% decrease in the MTS test and a 40% increase in the LDH test, while sCT-NA resulted to be harmless. These results are in line with those previously published by our group concerning the sCT-PFOs toxicity[15]. However, for the first time we observed that the cytotoxicity induced by sCT-PFOs was totally abolished in the presence of EPPS, in agreement with the results reported by Kim et al.[27] and Kim et al.[44], for another amyloid protein, which was Aβ. It's worth noting that EPPS has a protective effect against cytotoxicity induced by both amyloid proteins (sCT and Aβ).

The SDS-PAGE results indicated that pentamers, hexamers, heptamers and octamers were present only in the sCT-PFOs sample while were absent in the sCT-NA sample (Fig. 1B). Dimers, trimers and few tetramers were also present while monomers were absent in both samples. This is in good agreement with the NMR results published by Andreotti and Motta[41] indicating that, at pH 7.3, dimer is the stable form for sCT samples. This result demonstrates that the sCT toxic aggregates were pentamers, hexamers, heptamers and octamers while dimers, trimers and tetramers were non-toxic.

Notably, for the first time in our knowledge, we observed in the SDS-PAGE experiment that the presence of EPPS induced the disappearance of all aggregates, except dimers and trimers, in the PFO sample. Thus we demonstrated that EPPS, in 24 h, was able to disaggregate the pre-formed and/or hinder the formation of new metastable toxic species. This evidence can explain the protective effect exerted by EPPS on HT22-diff cell line (Fig. 2B,C).

The elution profile relative to the SEC column loaded with the sample aggregated for 24 h in the presence of EPPS (Fig. 1A red curve), showed a single and sharp peak different from the one observed without EPPS in the aggregation process. This demonstrates that EPPS leads to the formation of very low-MW aggregates (likely monomers and dimers). Thus, EPPS not only was able to disaggregate the pre-formed metastable toxic species (pentamers, hexamers, heptamers and octamers) but also to inhibit their formation, since the early stages.

Electrophysiology results regarding the synaptic response showed that treatment with the sCT-PFOs caused a dramatic effect on LTP induction, in the short- and long-term (Fig. 3). This has already been reported in our previous paper[32] and interpreted, in a biophysical work of our group[13], as due to the interaction of sCT-PFOs with the neuron membranes. In particular, we demonstrated that the interaction between the protein aggregates and the membrane was driven by electrostatic forces occurring between sCT and the sialic acids of GM1 present in the membrane. This caused membrane permeabilization and abnormal Ca^{2+}-influx responsible for the impaired synaptic transmission, depletion of synaptic vesicles resulting in synaptic silencing.

Notably, this didn't happen with sCT-NA samples[32,45,46]. Results we are reporting now confirm that sCT-NA didn't cause an alteration in LTP (Fig. 3).

The treatment with plain EPPS didn't induce significant differences in either LTP or any long-term differences (Fig. 3). Notably, our results are in good agreement with those published by Kim et al.[27], who orally administered plain EPPS in AD animal model.

Finally, we tested the effect of the mixed sample sCT-PFOs + EPPS. We detected, for the first time on our knowledge, that all PS amplitude values were equal to those of the control or higher than those measured with the sCT-NA sample. Notably, the toxic effect of sCT-PFOs sample resulted totally abolished by the presence of EPPS.

Summarizing the biological effects, EPPS protected from the amyloid toxicity induced by sCT-PFOs on both neuronal cells (HT22-diff) and learning memory model (murine hippocampal slices). More in particular, EPPS protected from the damage induced by pre-formed and metastable sCT-PFOs (pentamers, hexamers, heptamers and octamers).

It's well known that amyloid neurotoxicity is a membrane-based phenomenon. Thus, to investigate the molecular mechanism at the basis of the observed protective effect of EPPS, we applied the Z-potential technique to study the interaction of sCT-PFOs (and NA and Fs) with models of neuronal membranes (liposomes), in the presence and in the absence of EPPS. This technique gave information about the electrostatic properties of the sCT species and their change due to the interaction with liposomes, in the presence and in the absence of EPPS.

The sCT species, with and without EPPS

The measured Z-potential values of the plain sCT species were all negative (Fig. 4A). In particular, sCT-Fs resulted the most negative, the values relative to the sCT-PFOs the less negative and the Z-potential of the non-aggregated sample sCT-NA was in the middle (weakly negative).

Notably, the presence of EPPS altered only the value of the sCT-NA sample, doubling its negative value (Fig. 4A). This suggests that EPPS interacted only with the low-MW aggregates present in this sample, rendering them more negative. We speculate that in dimers, trimers and tetramers, abundant in the sCT-NA sample (Fig. 1B lane 5), the hydrophobic parts of the proteins were quite accessible to the solvent containing EPPS. Conversely, in the PFOs and Fs these parts were less or totally inaccessible.

Thus, we hypothesize that EPPS affected only the Z-potential value of the sample where the hydrophobic parts of the protein were accessible. This suggests that the interaction occurred between EPPS and the hydrophobic parts of the sCT. In particular, the fragment (CVLG) from 7 to 10 in the primary sequence with a maximum in the hydrophobicity scale in the 8th (V)[47].

The mixtures liposomes-sCT species, with and without EPPS

Concerning the Z-potential of the plain liposomes, we observe that all values were negative, as expected, and more negative in the presence of a high content of the negative GM1 (Fig. 4B). Notably, in the same figure we can see that the presence of EPPS didn't affect the Z-potential values of the plain GM1 high-content liposomes.

The occurrence of the sCT species together with high-content GM1 liposomes, without EPPS, affected the Z-potential values: NA and PFOs rendered less negative their values, while Fs didn't affect the Z-potential.

The occurrence of EPPS further modified the Z-potential: only the value of the sample containing sCT-NA takes a more negative value (Fig. 4B). This suggests that EPPS interacted only with the harmless dimers, trimers and tetramers (Fig. 1B lane 5), independently from the presence of liposomes, rendering them more and more negative with the result to stabilize them and inhibit their binding to the negative charged membranes.

Our Z-potential results indicated that EPPS was able to counteract both pathways of PFO formation in solution, which are "primary" and "secondary nucleation". It must be considered that the toxic aggregates are metastable and thus, at the equilibrium, the hindering of "primary" and "secondary nucleation" should reduce the abundance of the toxic species (sCT-PFOs) with the result to protect neurons from the membrane permeabilization.

In conclusion, the all body of our results can be interpreted by the fact that EPPS acted as a stabilizer of dimers, in agreement with the stability of dimers for sCT at pH 7.4 published by Andreotti and Motta[41]. Moreover, EPPS was able to disaggregate the pre-formed metastable toxic PFOs and to counteract the "primary nucleation" interacting with the hydrophobic parts of the sCT. At the same time, EPPS also inhibited the "secondary nucleation" triggered by the catalytic effects exerted by the surface of both mature fibres and/or lipid membranes. This is the reason why we observed that EPPS was able to strongly modify the sCT aggregation kinetics, hindering the formation of mature fibres (Fig. 5). This scenario can well explain the protective effects exerted by EPPS against the amyloid toxicity, evaluated in both in vitro and ex vivo models. However, in disagreement with the explanation proposed by Kim et al.[27], we didn't see an important disaggregation effect exerted by EPPS on the β-structure of Fs (only about 20% after about 800 h) (Fig. 6). This rules out the possibility that its protective effect could be ascribed to the direct disaggregation of pre-formed mature fibres.

Finally, we speculate that the recently proposed antibodies act on pre-formed fibres: Aducanumab coats the surface of the insoluble Fs[22] while Lecanemab bind proto-fibrils[24], with the result to form complexes quite big at molecular level (MWs higher than antibodies, which is 146 kDa for Aducanumab). In our opinion, this can be at the basis of the reported circulatory side effects[23]. Conversely, EPPS is a small molecule (MW 252 Da) that can't form big complexes in the interaction with sCT, ruling out the mentioned side effects.

Our data demonstrated that EPPS was a cheap and harmless substance able to protect neurons against the amyloid damage and could be an excellent candidate as a drug for the treatment of amyloid neurodegenerations. However, to definitely asses that EPPS at clinical relevant doses is actually effective and harmless, human trials sould be performed.

Materials and methods

Materials

sCT standard (MW 3.432 kDa) samples were purchased from European Pharmacopoeia, EDQM, France. 1-palmitoyl-2-oleoyl-*sn*-glycero-3-phosphocholine (POPC) was purchased from Avanti Polar Lipids (Alabaster, AL, USA); phosphate-buffered saline (PBS; 0.01 M phosphate buffer; 0.0027 M KCl; 0.137 M NaCl; pH 7.4) and

cholesterol (purity = 99%) were purchased from Sigma Aldrich. GM1, EPPS and ThT was purchased from Sigma Aldrich (E9502).

EPPS solution preparation

EPPS (MW 252.33 Da) 1 M solution was prepared by dissolving the powder in 5mM phosphate buffer (PB: PB 5mM, pH 7.4). For treatment to construct the Dose-Response curve HT22-diff cells were incubated in Hanks' Balanced Salt Solution (HBSS) (Life technologies) with EPPS at different concentrations. For combined treatment with PFOs on HT22 cells, EPPS was dissolved in N2-containing differentiation medium and incubated for 24 h before assessment of cell viability by MTS assay. For the electrophysiology experiments, EPPS was dissolved in artificial cerebral spinal fluid (ACSF) at a final concentration of 3mM.

Sample preparation of sCT by size exclusion chromatography (SEC)

We prepared a solutions of sCT at a concentration of 1mM, diluting 2 mg of sCT powder in 5mM phosphate buffer (PB: PB 5mM, pH 7.4). The solution was aggregated by incubation of for 24 h at room temperature. Then, the aggregated solution was loaded into the SEC column to purify the fractions enriched in oligomeric species. Short, samples were loaded into Sephadex G50-SEC column (GE HEALTHCARE, Milan, Italy - height: 500 mm, cross section: 20 mm). The column, which was maintained at 4 °C, was pre-equilibrated to the same ionic strength as the samples and calibrated with a solution containing standards: BSA 1 mg (66 kDa), Cytochrome c 1 mg (12.4 kDa-Combithek Boehringer, Mannheim, Germany), Aprotinin 1 mg (6.5 kDa), and Somatostatin 1 mg (1.63 kDa), suspended in PB buffer 5mM pH 7.4 and centrifuged at 15,700g× 10 min. sCT native fractions (0.5 mL aliquots) were eluted in absorption monitoring column at 280 nm by a variable wavelength UV detector (BIORAD Econo UV monitor, Hercules, CA, USA). The collected fractions (Gilson FC 203B, 1.4 mL/fraction) were administered directly into cell cultures to test their effects on cell viability and to mouse hippocampal slices to evaluate LTP.

To assess the effect exerted by EPPS, sCT at a concentration of 1mM (2 mg of sCT powder in 5mM PB) was incubated for 24 h in the presence of EPPS at a relative molar concentration of 1 sCT at 375 EPPS (used in the following biological tests).

Non-aggregated sCT solutions at a 1mM concentration, were prepared by dissolving sCT freeze-dried powder in desalinated water. For limiting the aggregation process, the solution was rapidly frozen and stored at − 80 °C.

Photo-induced cross-linking of unmodified proteins (PICUP) and tricine SDS-PAGE gel characterization

Aiming to obtain an electrophoretic characterization (tricine/SDS-PAGE) of the fraction eluted, samples were stabilized to prevent oligomers misfolding in a reducing environment. We therefore treated them for PICUP, a fixing procedure developed by Fancy and Kodadek[39] and applied by Bitan et al. to the study of metastable protein, without alteration of their original structure[40]. The original protocol was adapted by Diociauti et al.[15]. Briefly, for each sample, we prepared a 20 µL volume containing 80µM Oligomers, 50µM Tris (2,2 bipyridyl) dichlororuthenium (II) hexahydrate) and 1mM ammonium persulfate (SIGMA). Cross-linking reaction occurred irradiating samples for 2 s with a 100 W white lamp in a dark room, reaction was quickly quenched adding 20µL of reducing sample buffer containing 5% β-MOH and boiled for 5 min. Samples were finally analyzed by tricine/SDS-PAGE. Separating gel: 10% Acrylamide/Bis (32:1) (ICN Biomedicals, Inc., Aurora, Ohio USA/Fluka, Buchs, CH); spacer gel 6.5% Acrlamide/Bis and stacking gel: 2.5% Acrlamide/Bis. For each lane were run 40 µL of the sample buffer, or 8 µL of molecular weight markers (Color Marker Ultralow Range-SIGMA, cat n° C6210-1VL). Then, the gels were stained by silver procedure. Finally, gel band densitometry has been performed using the imaging freeware ImageJ. For each lane, grey-scale optical density profile has been obtained, including molecular weight markers (1.3 kDa, 3.5 kDa, 6.5 kDa, 14.4 kDa, 17.0 kDa, 26.6 kDa). Peaks corresponding to sCT prefibrillar oligomers: dimers, trimers, tetramers, pentamers and octamers have been individuated according to the molecular weight marker profile.

Liposome preparation

Liposomes were prepared according to the thin film hydration procedure, coupled with the freeze-thaw protocol and followed by extrusion. Briefly, the proper amounts of lipid stock solutions (POPC, Chol, and GM1) were mixed in a round bottom flask, to obtain the desired molar ratio: (i) GM1/POPC/Chol 4/48/48 for liposomes mimicking the whole neuronal membrane; (ii) GM1/POPC/Chol 50/25/25 for liposomes mimicking "lipid-rafts". Then, the solvent was removed by rotary evaporation (Buchi Rotavapor R-210; Buchi Vacuum controller V-800 R-200) to obtain the formation of a thin film on the bottom of the flask. The lipid film was kept overnight under reduced pressure (0.4 mbar) and then a proper amount of PBS was added to have a suspension of 0.7mM in total lipids. The suspension was vortex-mixed in order to completely detach the film from the flask, and the obtained multilamellar vesicles (MLVs) were freeze-thawed six times from liquid nitrogen to 60°C. MLVs were extruded ten times by a 10 mL Lipex Biomembranes extrusor, equipped with Whatman Nuclepore polycarbonate membrane (pore size 0.1 µm), to obtain small unilamellar vesicles (SUV) that were characterized for their size and Z-potential by DLS and electrophoretic mobility measurements, after dilution with PBS to a total lipid concentration of 0.124mM.

Cell cultures

HT22 cells were developed from their analogous HT4 cells, immortalized from primary mouse hippocampal neurons. HT22 cells were maintained at 37 °C, 10%, CO_2 in Dulbecco's modified Eagle's medium (DMEM, Sigma Aldrich–D6546) supplemented with 10% heat-inactivated FBS and kept at less than 50% of confluence.

Differentiation was carried out in NeuroBasal medium (NBM, Gibco, 21103-49) containing N2 supplement (Gibco-17502048), at least for 24–48 h before use.

Cytotoxicity assessed by MTS and LDH assay

MTS assay. Cell viability was assessed using CellTiter 96 AQueous One (Promega, USA), a chemosensitivity assay or a colorimetric method to determine the number of viable cells in proliferation. The CellTiter 96 AQueous Assay is composed by a novel tetrazolium compound, (3-(4,5-dimethylthiazol-2-yl)-5-(3-carboxymethoxyphenyl)-2-(4-sulfophenyl)-2 H- tetrazolium—MTS) and an electron-coupling reagent (phenazinemethosulfate—PMS). MTS is bioreduced by cells into a colored formazan product that is soluble in cell culture medium. The absorbance of the formazan at 490 nm can be measured directly from 96-well assay plates without additional processing[48]. In brief, 20 µL of MTS/PMS solution was added to 100 µL of HBSS in each well and incubated at 37°C for at least 2 h in a humidified, 10% CO_2 atmosphere. The conversion of MTS aqueous, soluble formazan is accomplished by dehydrogenase enzymes found in metabolically active cells. The quantity of formazan product as measured by the amount of 490 nm (Spark Multimode Microplate Reader, Tecan, Austria) absorbance is directly proportional to the number of living cells in culture.

LDH assay. Cytotoxicity was measured using LDH-Glo™ Cytotoxicity Assay (J2380, Promega, Madison, USA), which detects and quantifies lactate dehydrogenase (LDH) levels in the supernatant. LDH is a soluble and stable cytosolic enzyme present in many cell types, which is rapidly released into the cell culture medium after disruption of the plasma membrane, representing a widely used marker of cell toxicity. In the assay, LDH detection reagent (containing lactate, NAD^+, reductase, reductase substrate and Ultra-Glo™ rLuciferase) was added to a sample of diluted cell culture medium, as indicated by the manufacturer. If the sample contains LDH, the reactions coupled to the enzyme and proceeded simultaneously. The luminescent signal generated is proportional to the amount of LDH present in the sample. The biological effect is quantified by the Relative Luminiscence Unit % normalized to the control value. In detail, cells were plated at a density of 8×10^3 in a 96-well plate. At the end of treatment, for each well 4 µL of culture medium was taken and added to 46 µL of LDH storage buffer (TRIS-HCl 200mM pH 7.3, 10% Glycerol and 1% BSA) in a 96-well blank plate. To each well, 50 µL of LDH detection reagent (50 µL LDH Detection Enzyme Mix + 0.25 µL Reductase Substrate) was added, reaching the 25X dilution suggested by the manufacturer, and incubated for 60 min at 37°C. The luminescence of each sample was determined using a plate reader (Spark Multimode Microplate Reader-Tecan, Austria).

Extracellular recordings in mouse hippocampal slices

Male mice aged 10 to 14 weeks old, belonging to the strain BALB/c mice, purchased from Envigo S.r.l. (Udine, Italy), were used in accordance with ethics guidelines and regulations of the European Union Council Directive (86/609/ European Economic Community), FELASA (Federation of European Laboratory Animal Science Associations) guidelines and ARRIVE (Animal Research: Reporting of In Vivo Experiments) guidelines. All the experimental protocols were performed after approval of the project by the Italian Ministry of Public Health (authorization No. 86/2018-PR).

Briefly, all animals under anesthesia with halothane (2-Brom-2-chlor1,1,1-trifuor-ethan), were sacrificed minimizing their suffering. Their brains were quickly removed and placed in cold, oxygenated artificial cerebral spinal fluid (aCSF) containing the following (in mM): NaCl, 124; KCl, 2; KH_2PO_4, 1.25; $MgSO_4$, 2; $CaCl_2$, 2; $NaHCO_3$, 26; and glucose, 10. The hippocampus was rapidly dissected and cut transversely into 450 µm thick slices using a McIlwain tissue chopper (Mickle Laboratory Engineering Co., Gomshall, UK). Then, hippocampal slices were transferred to a tissue chamber, where they were laid in an interface between oxygenated ACSF and humidified gas (95% O_2, 5% CO2) at 32–34°C (pH = 7.4), constantly superfused at a flow rate of 1.2 mL/min[49].

Extracellular recordings of population spikes (PSs) were conducted in the pyramidal stratum of subfield CA1 hippocampal slices with glass microelectrodes filled with 2 M NaCl (resistance 5–10 MΩ). Orthodromic stimuli (10–500 mA, 20–90 ms, 0.1 Hz) were delivered through a platinum electrode placed in the stratum radiatum in the collateral/commissural pathways of Schaffer CA1. The intensity of the test stimulus of 50 ms square pulses was adjusted to elicit a PS of 2–3 mV at 0.03 Hz. Every minute PS amplitude was calculated as the average of six recordings made every 10s. After recording stable signals (15–20 min), hippocampal slices were treated with EPPS (3mM) solution for 60 min and/or non aggregated sCT or PFOs-enriched sCT solutions to test their respective effects on basal synaptic transmission. PFOs and non-aggregated were diluted in ACSF carboxygenate to a final concentration of around 8µM and used to perfuse the slices. Subsequently, a tetanic stimulation (100 Hz, 1 s) was delivered to induce LTP at the same stimulus intensity used for baseline responses. Field potentials were fed to a computer interface (Digidata 1440 A, Axon Instruments, Foster City, CA, USA) for subsequent analysis with PCLAMP10 software (Axon Instruments).

Electrophoretic mobility and Z-potential

Electrophoretic mobility measurements were performed by a Malvern Nano-ZetaSizer. Analysis of the Doppler shift was done by using phase analysis light scattering (PALS)[50]. This method is especially useful for samples with low mobilities. The mobility µ of the liposomes is converted into a Z-potential using the Smoluchowski relation $Z = \mu\, \eta/\varepsilon$, where ε and η are the permittivity and the viscosity of the solution, respectively. Measurements have been performed in a thermostatted cell; temperature was fixed at 25°C.

In the Z-potential experiments, mixed liposomes and sCT-samples were prepared by adding 131 µL of 80µM sCT (NA, PFOs, fibers, dissolved in 5mM PB) to 169 µl of 0.124mM liposomes, to obtain a final lipid concentration of 0.07mM as in our previous investigation[43]. 5mM PB was used for preparation of control samples. To evaluate the effect of EPPS on the interaction between the cellular models and sCT aggregates, a proper volume of EPPS 200mM was added to liposomes suspension, before addition of sCT, to have 3mM as final EPPS concentration.

ThT aggregation assay

sCT at a concentration of 1mM was used for ThT fluorescence experiments. Samples were prepared in the wells of (100 μL) of a 96-wells dark plate (Corning Low Volume 384) and were obtained mixing 1mM sCT stock solution with 3mM ThT. The mixture was stirred continuously at 25°C and its fluorescence was recorded in triplicate (excitation: $\lambda = 440$ nm, emission: $\lambda = 535$ nm) by using a VICTOR Multilabel Plate Reader plate spectrofluorometer equipped with a temperature-controlled cell holder. Measurements were performed in triplicate and blank values in triplicate (3mM ThT in 5mM PB), were subtracted. Errors were expressed as the sum of standard errors obtained for the three samples containing sCT and the three relative blanks.

Statistical analysis

Statistical analysis was performed using GraphPad Prism 8 Software (Prism 8.0.1, La Jolla, CA, USA). Cellular viability estimations for each experimental condition were obtained in quadruplicate, and data were normalized with respect to controls. A multiple comparison in cellular viability was obtained by ANOVA and the Dunnett Test, with a confidence level of 95% and 99%. For electrophysiological experiments, data were expressed as mean ± SEM, and n represented the number of slices analyzed. Data were compared with ANOVA and Tukey's Multiple Comparison Test and were considered significantly different if $p < 0.05$.

Data availability

Data availability The datasets used and/or analyzed during the current study are available from the corresponding author on reasonable request.

Received: 31 May 2024; Accepted: 25 October 2024
Published online: 03 November 2024

References

1. Ross, C. A. & Poirier, M. A. Protein aggregation and neurodegenerative disease. *Nat. Med.* **10**(Suppl), S10 (2004).
2. Soto, C. & Pritzkow, S. Protein misfolding, aggregation, and conformational strains in neurodegenerative diseases. *Nat. Neurosci.* **21**, 1332–1340 (2018).
3. Gao, J. et al. Abnormalities of mitochondrial dynamics in neurodegenerative diseases. *Antioxidants (Basel)* **6** (2017).
4. Rey, F., Ottolenghi, S., Zuccotti, G., Samaja, M. & Carelli, S. Mitochondrial dysfunctions in neurodegenerative diseases: Role in disease pathogenesis, strategies for analysis and therapeutic prospects. *Neural Regen Res.* **17**, 754–758 (2022).
5. Haass, C. & Selkoe, D. J. Soluble protein oligomers in neurodegeneration: Lessons from the Alzheimer's amyloid beta-peptide. *Nat. Rev. Mol. Cell. Biol.* **8**, 101–112 (2007).
6. Chiti, F. & Dobson, C. M. Protein & misfolding amyloid formation, and human disease: A summary of progress over the last decade. *Annu. Rev. Biochem.* **86**, 27–68 (2017).
7. Glabe, C. G. Common mechanisms of amyloid oligomer pathogenesis in degenerative disease. *Neurobiol. Aging.* **27**, 570–575 (2006).
8. Ye, Y. Regulation of protein homeostasis by unconventional protein secretion in mammalian cells. *Semin Cell. Dev. Biol.* **83**, 29–35 (2018).
9. Sipe, J. D. Amyloidosis. *Crit. Rev. Clin. Lab. Sci.* **31**, 325–354 (1994).
10. Aigelsreiter, A. et al. How a cell deals with abnormal proteins. Pathogenetic mechanisms in protein aggregation diseases. *Pathobiology* **74**, 145–158 (2007).
11. Dogan, A. Amyloidosis: Insights from proteomics. *Annu. Rev. Pathol.* **12**, 277–304 (2017).
12. Kurtishi, A., Rosen, B., Patil, K. S., Alves, G. W. & Møller, S. G. Cellular proteostasis in neurodegeneration. *Mol. Neurobiol.* **56**, 3676–3689 (2019).
13. Diociaiuti, M. et al. The Interaction between amyloid prefibrillar oligomers of salmon calcitonin and a lipid-raft model: Molecular mechanisms leading to membrane damage, Ca 2+-influx and neurotoxicity. *Biomolecules* **10** (2019).
14. Benilova, I., Karran, E. & De Strooper, B. The toxic Aβ oligomer and Alzheimer's disease: An emperor in need of clothes. *Nat. Neurosci.* **15**, 349–357 (2012).
15. Diociaiuti, M. et al. Native metastable prefibrillar oligomers are the most neurotoxic species among amyloid aggregates. *Biochim. Biophys. Acta Mol. Basis Dis.* **1842**, 1622–1629 (2014).
16. Diociaiuti, M., Bonanni, R., Cariati, I. & Frank, C. & D'arcangelo, G. Amyloid prefibrillar oligomers: The surprising commonalities in their structure and activity. *Int. J. Mol. Sci.* **22** (2021).
17. Malchiodi-Albedi, F., Paradisi, S., Matteucci, A., Frank, C. & Diociaiuti, M. Amyloid oligomer neurotoxicity, calcium dysregulation, and lipid rafts. *Int. J. Alzheimer's Dis.* **2011**, 906964 (2011).
18. Vetri, V. & Foderà, V. The route to protein aggregate superstructures: Particulates and amyloid-like spherulites. *FEBS Lett.* **589**, 2448–2463 (2015).
19. Stefani, M. Biochemical and biophysical features of both oligomer/fibril and cell membrane in amyloid cytotoxicity. *FEBS J.* **277**, 4602–4613 (2010).
20. Banerjee, S. & Lyubchenko, Y. L. Interaction of amyloidogenic proteins with membranes and molecular mechanism for the development of Alzheimer's disease. *Alzheimers Res. Ther. Open. Access.* **2**, 1 (2019).
21. Cohen, S. I. A. et al. Proliferation of amyloid-β42 aggregates occurs through a secondary nucleation mechanism. *Proc. Natl. Acad. Sci. U S A* **110**, 9758–9763 (2013).
22. Linse, S. et al. Kinetic fingerprints differentiate the mechanisms of action of anti-Aβ antibodies. *Nat. Struct. Mol. Biol.* **27**, 1125–1133 (2020).
23. Knopman, D. S., Jones, D. T. & Greicius, M. D. Failure to demonstrate efficacy of aducanumab: An analysis of the EMERGE and ENGAGE trials as reported by Biogen, December 2019. *Alzheimer's Dement.* **17**, 696–701 (2021).
24. Söderberg, L. et al. Lecanemab, aducanumab, and gantenerumab - binding profiles to different forms of amyloid-beta might explain efficacy and side effects in clinical trials for Alzheimer's disease. *Neurotherapeutics* **20**, 195–206 (2023).
25. CHMP. What were the main reasons for refusing the marketing authorisation?.
26. van Dyck, C. H. C. J. S. P. A. Lecanemab in Early Alzheimer's Disease.
27. Kim, H. Y. et al. EPPS rescues hippocampus-dependent cognitive deficits in APP/PS1 mice by disaggregation of amyloid-β oligomers and plaques. *Nat. Commun.* **6**, 8997 (2015).
28. Kamgar-Parsi, K. et al. Structural biology of calcitonin: From aqueous therapeutic properties to amyloid aggregation. *Isr. J. Chem.* **57**, 634–650 (2017).

29. Diociaiuti, M., Gaudiano, M. C. & Malchiodi-Albedi, F. The slowly aggregating salmon Calcitonin: A useful tool for the study of the amyloid oligomers structure and activity. *Int. J. Mol. Sci.* **12**, 9277–9295 (2011).
30. Kayed, R. & Lasagna-Reeves, C. A. Molecular mechanisms of amyloid oligomers toxicity. *J. Alzheimers Dis.* **33**(Suppl 1) (2013).
31. Xu, S. Cross-beta-sheet structure in amyloid fiber formation. *J. Phys. Chem. B* **113**, 12447–12455 (2009).
32. Belfiore, M. et al. Calcitonin native prefibrillar oligomers but not monomers induce membrane damage that triggers NMDA-mediated Ca(2+)-influx, LTP impairment and neurotoxicity. *Sci. Rep.* **9**, 5144 (2019).
33. He, M., Liu, J., Cheng, S., Xing, Y. & Suo, W. Z. Differentiation renders susceptibility to excitotoxicity in HT22 neurons. *Neural Regen. Res.* **8**, 1297–1306 (2013).
34. London, E. Insights into lipid raft structure and formation from experiments in model membranes. *Curr. Opin. Struct. Biol.* **12**, 480–486 (2002).
35. Simons, K. & Toomre, D. Lipid rafts and signal transduction. *Nat. Rev. Mol. Cell. Biol.* **1**, 31–39 (2000).
36. Manna, M. & Mukhopadhyay, C. Binding, conformational transition and dimerization of amyloid-β peptide on GM1-containing ternary membrane: Insights from molecular dynamics simulation. *PLoS ONE* **8** (2013).
37. Fantini, J., Yahi, N. & Garmy, N. Cholesterol accelerates the binding of Alzheimer's β-amyloid peptide to ganglioside GM1 through a universal hydrogen-bond-dependent sterol tuning of glycolipid conformation. *Front. Physiol.* **4** (2013).
38. De Meulenaer, B., Van Der Meeren, P., De Cuyper, M., Vanderdeelen, J. & Baert, L. Electrophoretic and dynamic light scattering study of the interaction of cytochrome c with dimyristoylphosphatidylglycerol, dimyristoylphosphatidylcholine, and intramembranously mixed liposomes. *J. Colloid Interface Sci.* **189**, 254–258 (1997).
39. Fancy, D. A. & Kodadek, T. Chemistry for the analysis of protein-protein interactions: Rapid and efficient cross-linking triggered by long wavelength light. *Proc. Natl. Acad. Sci. U S A* **96**, 6020–6024 (1999).
40. Bitan, G. Structural study of metastable amyloidogenic protein oligomers by photo-induced cross-linking of unmodified proteins. *Methods Enzymol.* **413**, 217–236 (2006).
41. Andreotti, G. & Motta, A. Modulating calcitonin fibrillogenesis: An antiparallel alpha-helical dimer inhibits fibrillation of salmon calcitonin. *J. Biol. Chem.* **279**, 6364–6370 (2004).
42. Cariati, I. et al. Role of electrostatic interactions in calcitonin prefibrillar oligomer-induced amyloid neurotoxicity and protective effect of neuraminidase. *Int. J. Mol. Sci.* **22** (2021).
43. Diociaiuti, M. et al. Monosialoganglioside-GM1 triggers binding of the amyloid-protein salmon calcitonin to a Langmuir membrane model mimicking the occurrence of lipid-rafts. *Biochem. Biophys. Rep.* **8**, 365–375 (2016).
44. Kim, H. Y., Kim, Y., Han, G. & Kim, D. J. Regulation of in vitro Aβ1–40 aggregation mediated by small molecules. *J. Alzheimers Dis.* **22**, 73–85 (2010).
45. Kayed, R. et al. Common structure of soluble amyloid oligomers implies common mechanism of pathogenesis. *Science.* **300**, 486–489 (2003).
46. Kayed, R. et al. Permeabilization of lipid bilayers is a common conformation-dependent activity of soluble amyloid oligomers in protein misfolding diseases. *J. Biol. Chem.* **279**, 46363–46366 (2004).
47. Diociaiuti, M., Fioravanti, R. & Belfiore, M. Neurotoxic amyloid prefibrillar oligomers: Do salmon calcitonin and amyloid β1–42 wear the same outfit? *Arch. Clin. Toxicol. (Middlet)* **2**, (2021).
48. Barltrop, J. A., Owen, T. C., Cory, A. H. & Cory, J. G. 5-(3-carboxymethoxyphenyl)-2-(4,5-dimethylthiazolyl)-3-(4-sulfophenyl) tetrazolium, inner salt (MTS) and related analogs of 3-(4,5-dimethylthiazolyl)-2,5-diphenyltetrazolium bromide (MTT) reducing to purple water-soluble formazans As cell-viability indicators. *Bioorg. Med. Chem. Lett.* **1**, 611–614 (1991).
49. Palmieri, M. et al. Effects of short-term aerobic exercise in a mouse model of Niemann-Pick type C disease on synaptic and muscle plasticity. *Ann. Ist Super Sanità.* **55**, 330–337 (2019).
50. Tscharnuter, W. W. Mobility measurements by phase analysis. *Appl. Opt.* **40**, 7–9 (2001).

Acknowledgements

HT22 cell line was kindly gifted from David Schubert of "The Salk Institute", La Jolla, CA (USA). C.G., C.B., M.D. are grateful to the Consiglio Nazionale delle Ricerche (CNR, Rome - Italy) and Universidad de Antioquia (Medellín - Colombia) for the support given to the project n.2024-68170 entitled:" The study of the protective effect exerted by 4-(2-hydroxyethyl)-1-piperazinepropanesulphonic acid (EPPS) on neurodegeneration induced by prefibrillar salmon Calcitonin (sCT) amyloid oligomers" stipulated between the Institute for Biological System of Consiglio Nazionale delle Ricerche (ISB-CNR) and Universidad de Antioquia, within the cooperation framework agreement (MOU) n° 005-2022.

Author contributions

Conceptualization B.Z., C.G., C.F., V.T., M.D., G.D. Designed the experiments B.Z., R.B., I.C., S.S., C.B., M.D., G.D Performed citotoxicity experiments R.B., M.B., M.G.S. Performed plasticity experiments B.Z Performed protein sample preparation and characterization experiments M.B., M.G.S., R.F., G.C. Biophysical experiments S.S., C.B., M.D., G.C. Writing-Original Draft preparation, B.Z., M.D. Writing-Review and Editing, B.Z., C.F., V.T., G.D., M.D. Super-vision, M.D., G.D. All authors approved the final manuscript.

Funding

This work was supported by the Italian "Ministero della Salute" with the "Progetto Ordinario di Ricerca Finalizzata (RF-2013-02355682)" entitled: "Calcitonin oligomers as a model to study the amyloid neurotoxicity: the focal role played by lipid rafts in the prevention and cure".

Declarations

Competing interests

The authors declare no competing interests.

Additional information

Supplementary Information The online version contains supplementary material available at https://doi.org/10.1038/s41598-024-77859-9.

Correspondence and requests for materials should be addressed to M.D.